

Anisotropic nonrelativistic charge-to-spin conversion in altermagnets

Mingbo Dou,¹ Xianjie Wang,^{1,2} and L. L. Tao^{1,2,*}

¹*School of Physics, Harbin Institute of Technology, Harbin 150001, China*

²*Heilongjiang Provincial Key Laboratory of Advanced Quantum Functional Materials and Sensor Devices, Harbin 150001, China*

(Dated: December 10, 2025)

The charge-to-spin conversion provides an efficient way to manipulate the magnetization by electrical means. In this work, we report on a study on the anisotropic nonrelativistic charge-to-spin conversion response to the current direction in altermagnets. Based on the general group-theoretical analysis, we derive analytical formulas for the anisotropic conversion ratio and identify its maximum value. We then exemplify those phenomena in representative altermagnets based on the density functional theory calculations. The highly anisotropic charge-to-spin conversion efficiency, varying from zero to several tens of percent, was demonstrated. Our work shines more light on the exploration of the nonrelativistic generation of spin currents in altermagnets.

I. INTRODUCTION

The generation of spin currents through the charge-to-spin conversion by electrical means is of vital importance in spintronics[1–4]. Spin (polarized) currents can exert spin torques including spin-transfer torque (STT)[5–8] and spin-orbit torque (SOT)[9–14] that may lead to the current-induced magnetization switching crucial for lower-power spintronic devices[15–17]. It is known that the spin-polarized current responsible for the STT is odd under the time reversal \mathcal{T} while the spin current responsible for the SOT is even under \mathcal{T} . Despite significant advances in STT and SOT based spintronic devices, the inherent deficiencies have limited the further development of the spin-torque devices such as non-volatile magnetic random-access memories[15–17]. For example, the spin current induced by the spin Hall effect[1] or the Rashba effect[18, 19] is largely based on the strength of spin-orbit coupling (SOC), which is rather small as compared to the magnetic exchange field. Moreover, the SOC induced spin current typically reveals the in-plane spin polarization, which is not favorable to switch the perpendicular magnetization[15–17, 20].

Recently, the spin-splitter torque (SST)[21] based on the spin-splitter effect was theoretically proposed in altermagnets[22–26] endowed with the zero net magnetization and sizable nonrelativistic spin splitting on the order of 1 eV[27, 28]. As distinct from the SOT, the spin current responsible for the SST is induced by the nonrelativistic spin splitting and is odd under \mathcal{T} [21]. Moreover, the spin polarization parallel to the Néel vector is highly controllable promising for the perpendicular magnetization switching[20]. A highly charge-to-spin conversion ratio of $\sim 28\%$ was theoretically predicted in the altermagnet RuO₂[21] and the SST with high efficiency was later observed in the RuO₂ films[29–31]. It was found that the direction of spin current strongly depends on the crystal orientation while the spin polarization is parallel to the Néel vector[29]. Moreover, the field-free switching of the perpendicular magnetization of the Co layer via the SST exerted by the spin current of the RuO₂ layer was achieved at room temperature[30].

On the other hand, the charge-to-spin conversion is expected to show anisotropy for different current directions, as evidenced by the anisotropic spin Hall effect in nonmagnetic hcp metals[32] and anisotropic charge-spin conversion in the topological semimetal SrIrO₃[33]. For altermagnets, the highly anisotropic Fermi surface due to significant spin-split bands is expected to give rise to the anisotropic charge-to-spin conversion for the current along different crystal orientations. This has been partially supported by the different polarized spin currents in the different crystal planes of the RuO₂[29, 30]. However, the systematic study on the anisotropic spin current for all altermagnets remains largely unexplored. In particular, the spatial anisotropy and analytical formulas for the nonrelativistic charge-to-spin conversion remains to be studied. It is the purpose of this work to explore the anisotropic charge-to-spin conversion and identify the crystal orientation sustaining the maximum conversion efficiency for different altermagnets.

The rest of the paper is organized as follows. In Sec. II, we present the theoretical formalism for the spin current and charge-to-spin conversion ratio calculations. In Sec. III, we discuss the anisotropy of charge-to-spin conversion based on the general symmetry analysis. In Sec. IV, we present the DFT results for representative altermagnets. Finally, Sec. V is reserved for further discussion and conclusion.

II. THEORETICAL FORMALISM

Assume that a system is subject to an external electric field \mathcal{E} . To first order in \mathcal{E} , the spin current density \mathbf{J}_s (second-rank tensor) takes the form[34]

$$J_{sj}^i = \sigma_{jk}^i \mathcal{E}_k, \quad (1)$$

where the spin conductivity σ_{jk}^i (third-rank tensor) describes that a charge current along the k direction induces a spin current along the j direction with spin polarization along the i direction. The indices $i, j, k = x, y, z$ denote Cartesian components and a summation over repeated indices is understood. Within the linear response theory using the Kubo formalism and the relaxation time $\tau = \hbar/2\Gamma$ approximation, two princi-

* Contact author: lltao@hit.edu.cn

pal contributors to σ_{jk}^i are the \mathcal{T} -odd contribution[35–37]

$$\sigma_{jk}^{\text{odd},i} = -\frac{e\hbar}{\pi} \sum_{\mathbf{k},m,n} \frac{\text{Re}[\langle\psi_{n\mathbf{k}}|\mathcal{J}_j^i|\psi_{m\mathbf{k}}\rangle\langle\psi_{m\mathbf{k}}|v_k|\psi_{n\mathbf{k}}\rangle]\Gamma^2}{[(\epsilon_F - \epsilon_{n\mathbf{k}})^2 + \Gamma^2][(\epsilon_F - \epsilon_{m\mathbf{k}})^2 + \Gamma^2]}, \quad (2)$$

and the \mathcal{T} -even contribution ($\Gamma \rightarrow 0$)

$$\sigma_{jk}^{\text{even},i} = -2e\hbar \sum_{\mathbf{k},m \neq n} \frac{\text{Im}[\langle\psi_{n\mathbf{k}}|\mathcal{J}_j^i|\psi_{m\mathbf{k}}\rangle\langle\psi_{m\mathbf{k}}|v_k|\psi_{n\mathbf{k}}\rangle]}{(\epsilon_{n\mathbf{k}} - \epsilon_{m\mathbf{k}})^2}, \quad (3)$$

where $\mathcal{J}_j^i = \hbar\{\sigma_i, v_j\}/4$ is the spin current operator given in terms of spin (velocity) operator σ_i (v_j) and the reduced Planck's constant \hbar , ϵ_F the Fermi energy, Γ the broadening parameter, and $\psi_{n\mathbf{k}}$ ($\epsilon_{n\mathbf{k}}$) the Bloch function (energy eigenvalue) of the n th band. In Eq. (3), the summation index m (n) is restricted to unoccupied (occupied) bands. In this work, we consider the nonrelativistic charge-to-spin conversion in altermagnets characterized by $\sigma_{jk}^{\text{odd},i}$ due to that $\sigma_{jk}^{\text{even},i}$ vanishes without SOC. Thus, the superscript “odd” in $\sigma_{jk}^{\text{odd},i}$ is to be omitted in the following. In the limit of $\Gamma \rightarrow 0$, namely small broadening, Eq. (2) is reduced to[35]

$$\sigma_{jk}^i = -e\tau \sum_{\mathbf{k}n} \langle\psi_{n\mathbf{k}}|\mathcal{J}_j^i|\psi_{n\mathbf{k}}\rangle\langle\psi_{n\mathbf{k}}|v_k|\psi_{n\mathbf{k}}\rangle\delta(\epsilon_F - \epsilon_{n\mathbf{k}}). \quad (4)$$

Note that, in the case of altermagnets with collinear spin configuration that ignores SOC, Eq. (4) can be expressed in

closed form in terms of the electrical conductivity

$$\sigma_{jk}^i = -\frac{\hbar}{2e}(\bar{\sigma}_{jk}^\uparrow - \bar{\sigma}_{jk}^\downarrow) \cos \alpha, \quad (5)$$

where α is the angle between the Néel vector and the i -axis, \uparrow, \downarrow are the spin indices with the spin quantization axis along the Néel vector and, the spin-resolved electrical conductivity $\bar{\sigma}_{ij}^s$ ($s = \uparrow, \downarrow$) in the zero-temperature limit reads[38–40]

$$\bar{\sigma}_{ij}^s(\epsilon_F) = e^2\tau \sum_{\mathbf{k}n} v_{\mathbf{k}i}^{ns} v_{\mathbf{k}j}^{ns} \delta(\epsilon_F - \epsilon_{n\mathbf{k}}). \quad (6)$$

It is to be noted that the spin polarization i is dictated by the Néel vector orientation. For example, when the Néel vector is along the z direction, we have $i = z$. With the Néel vector being in the $x - y$ plane, we have $i = x, y$, and so forth.

It follows from Eq. (5) that, in addition to $\alpha \neq \pi/2$, the nonzero σ_{jk}^i requires that $\bar{\sigma}_{jk}^\uparrow \neq \bar{\sigma}_{jk}^\downarrow$, which can be determined in advance from symmetry arguments, as demonstrated recently[41]. Given the fact that the conductivity components for the g -wave and i -wave altermagnets are spin degenerate[41], we focus on the d -wave altermagnet throughout this work. For an applied electric field \mathcal{E} along the direction $\hat{\mathbf{n}} = (\sin \theta \cos \varphi, \sin \theta \sin \varphi, \cos \theta)$ (θ for polar angle and φ for azimuthal angle), on combining Eqs. (1) and (5), we have

$$\begin{pmatrix} J_{sx}^i \\ J_{sy}^i \\ J_{sz}^i \end{pmatrix} = -\frac{\hbar \cos \alpha}{2e} \begin{pmatrix} (\bar{\sigma}_{xx}^\uparrow - \bar{\sigma}_{xx}^\downarrow) \sin \theta \cos \varphi + (\bar{\sigma}_{xy}^\uparrow - \bar{\sigma}_{xy}^\downarrow) \sin \theta \sin \varphi + (\bar{\sigma}_{xz}^\uparrow - \bar{\sigma}_{xz}^\downarrow) \cos \theta \\ (\bar{\sigma}_{xy}^\uparrow - \bar{\sigma}_{xy}^\downarrow) \sin \theta \cos \varphi + (\bar{\sigma}_{yy}^\uparrow - \bar{\sigma}_{yy}^\downarrow) \sin \theta \sin \varphi + (\bar{\sigma}_{yz}^\uparrow - \bar{\sigma}_{yz}^\downarrow) \cos \theta \\ (\bar{\sigma}_{xz}^\uparrow - \bar{\sigma}_{xz}^\downarrow) \sin \theta \cos \varphi + (\bar{\sigma}_{yz}^\uparrow - \bar{\sigma}_{yz}^\downarrow) \sin \theta \sin \varphi + (\bar{\sigma}_{zz}^\uparrow - \bar{\sigma}_{zz}^\downarrow) \cos \theta \end{pmatrix} \mathcal{E} = \boldsymbol{\sigma}(\theta, \varphi) \mathcal{E}, \quad (7)$$

where $\boldsymbol{\sigma}(\theta, \varphi)$ is a three-by-one column vector. From Eq. (7), one can specify the spin-current direction $\hat{\mathbf{J}}_s$ and the anisotropic spin conductivity $\boldsymbol{\sigma}(\theta, \varphi)$. In addition, the conductivity along the direction $\hat{\mathbf{n}}$ is given by[41]

$$\bar{\sigma}(\theta, \varphi) = \bar{\sigma}_{xx} \sin^2 \theta \cos^2 \varphi + \bar{\sigma}_{yy} \sin^2 \theta \sin^2 \varphi + \bar{\sigma}_{zz} \cos^2 \theta + \bar{\sigma}_{xy} \sin^2 \theta \sin(2\varphi) + \bar{\sigma}_{yz} \sin(2\theta) \sin \varphi + \bar{\sigma}_{xz} \sin(2\theta) \cos \varphi, \quad (8)$$

where we have used the fact that $\bar{\sigma}_{ij} = \bar{\sigma}_{ij}^\uparrow + \bar{\sigma}_{ij}^\downarrow$. Then, on combining Eqs. (7) and (8), we introduce the anisotropic charge-to-spin conversion ratio $\Theta(\theta, \varphi)$ as

$$\Theta(\theta, \varphi) = \frac{e}{\hbar} \frac{|\boldsymbol{\sigma}(\theta, \varphi)|}{\bar{\sigma}(\theta, \varphi)}. \quad (9)$$

Without loss of generality, $\alpha = 0$ in Eq. (7) will be used in

the following.

III. GROUP-THEORETICAL ANALYSIS

We first analyze the anisotropic charge-to-spin conversion by use of the general symmetry analysis. It has been established that the altermagnet can be described by the third type of spin point groups (SPGs)[22, 23]. As mentioned above, only the d -wave altermagnet sustains the spin-polarized conductivity and the corresponding SPGs are $^{22}/^2m$, $^{2m^2}m^1m$, $^{24}/^1m$, and $^{24}/^1m^2m^1m$ [22, 23], as listed in Table I. For the SPG $^{22}/^2m$, the spin-polarized conductivity components are $\bar{\sigma}_{xy}$ and $\bar{\sigma}_{yz}$ [41]. From Eq. (7), the spin-current direction $\hat{\mathbf{J}}_s$ can be obtained as

$$\hat{\mathbf{J}}_s = -\frac{\bar{\sigma}_{xy}^\uparrow \sin \theta \sin \varphi \hat{\mathbf{x}} + (\bar{\sigma}_{xy}^\uparrow \sin \theta \cos \varphi + \bar{\sigma}_{yz}^\uparrow \cos \theta) \hat{\mathbf{y}} + \bar{\sigma}_{yz}^\uparrow \sin \theta \sin \varphi \hat{\mathbf{z}}}{\sqrt{(\bar{\sigma}_{xy}^\uparrow \sin \theta)^2 + (\bar{\sigma}_{yz}^\uparrow \cos \theta)^2 + (\bar{\sigma}_{yz}^\uparrow \sin \theta \sin \varphi)^2 + \bar{\sigma}_{xy}^\uparrow \bar{\sigma}_{yz}^\uparrow \sin(2\theta) \cos \varphi}}, \quad (10)$$

TABLE I. Symmetry allowed nonrelativistic spin conductivity tensors σ_{jk}^i ($i, j, k = x, y, z$) and $\hat{\mathbf{n}}$ -dependent spin-current direction $\hat{\mathbf{J}}_s$ for different SPGs sustaining the d -wave altermagnet.

SPG	σ_{jk}^i ($i, j, k = x, y, z$)	$\hat{\mathbf{J}}_s$ ($\hat{\mathbf{n}} \hat{\mathbf{x}}$)	$\hat{\mathbf{J}}_s$ ($\hat{\mathbf{n}} \hat{\mathbf{y}}$)	$\hat{\mathbf{J}}_s$ ($\hat{\mathbf{n}} \hat{\mathbf{z}}$)	Candidate
$2^2/2m$	$\sigma_{xy}^i, \sigma_{yz}^i$	$-\text{sgn}(\bar{\sigma}_{xy}^\uparrow)\hat{\mathbf{y}}$	$-\frac{\bar{\sigma}_{xy}^\uparrow\hat{\mathbf{x}}+\bar{\sigma}_{yz}^\uparrow\hat{\mathbf{z}}}{\sqrt{(\bar{\sigma}_{xy}^\uparrow)^2+(\bar{\sigma}_{yz}^\uparrow)^2}}$	$-\text{sgn}(\bar{\sigma}_{yz}^\uparrow)\hat{\mathbf{y}}$	CuF ₂
$2^2m^2m^1m$	σ_{xy}^i	$-\text{sgn}(\bar{\sigma}_{xy}^\uparrow)\hat{\mathbf{y}}$	$-\text{sgn}(\bar{\sigma}_{xy}^\uparrow)\hat{\mathbf{x}}$	-	FeSb ₂
$2^4/1m$	$\sigma_{xx}^i, \sigma_{yy}^i, \sigma_{xy}^i$	$-\frac{(\bar{\sigma}_{xx}^\uparrow-\bar{\sigma}_{xx}^\downarrow)\hat{\mathbf{x}}+2\bar{\sigma}_{xy}^\uparrow\hat{\mathbf{y}}}{\sqrt{(\bar{\sigma}_{xx}^\uparrow-\bar{\sigma}_{xx}^\downarrow)^2+4(\bar{\sigma}_{xy}^\uparrow)^2}}$	$-\frac{2\bar{\sigma}_{xy}^\uparrow\hat{\mathbf{x}}-(\bar{\sigma}_{xx}^\uparrow-\bar{\sigma}_{xx}^\downarrow)\hat{\mathbf{y}}}{\sqrt{(\bar{\sigma}_{xx}^\uparrow-\bar{\sigma}_{xx}^\downarrow)^2+4(\bar{\sigma}_{xy}^\uparrow)^2}}$	-	KRu ₄ O ₈
$2^4/1m^2m^1m$	σ_{xy}^i	$-\text{sgn}(\bar{\sigma}_{xy}^\uparrow)\hat{\mathbf{y}}$	$-\text{sgn}(\bar{\sigma}_{xy}^\uparrow)\hat{\mathbf{x}}$	-	RuO ₂

and the conversion ratio Θ can be obtained from Eq. (9) as

$$\Theta = \frac{\sqrt{(\bar{\sigma}_{xy}^\uparrow \sin \theta)^2 + (\bar{\sigma}_{yz}^\uparrow \cos \theta)^2 + (\bar{\sigma}_{yz}^\uparrow \sin \theta \sin \varphi)^2 + \bar{\sigma}_{xy}^\uparrow \bar{\sigma}_{yz}^\uparrow \sin(2\theta) \cos \varphi}}{\bar{\sigma}_{xx} \sin^2 \theta \cos^2 \varphi + \bar{\sigma}_{yy} \sin^2 \theta \sin^2 \varphi + \bar{\sigma}_{zz} \cos^2 \theta + \bar{\sigma}_{xz} \sin(2\theta) \cos \varphi}. \quad (11)$$

$\hat{\mathbf{J}}_s$ for different $\hat{\mathbf{n}}$ can be immediately inferred from Eq. (10). In Table I, we summarize $\hat{\mathbf{J}}_s$ when $\hat{\mathbf{n}}$ is along one of the three principal axes. For $\hat{\mathbf{n}}||\hat{\mathbf{x}}$ and $\hat{\mathbf{n}}||\hat{\mathbf{z}}$, $\hat{\mathbf{J}}_s$ is along the y direction as expected from the nonzero components σ_{xy}^i and σ_{yz}^i . For $\hat{\mathbf{n}}||\hat{\mathbf{y}}$, $\hat{\mathbf{J}}_s$ is in the $x-z$ plane. On the other hand, the extrema of Θ can be determined in principle from that $\partial\Theta/\partial\theta = 0$ and $\partial\Theta/\partial\varphi = 0$. However, the result is too complicated to evaluate analytically. This has to be analyzed by numerical methods.

For the SPG $2^2m^2m^1m$, only $\bar{\sigma}_{xy}$ is spin polarized[41]. Similarly, we have

$$\hat{\mathbf{J}}_s = -\text{sgn}(\bar{\sigma}_{xy}^\uparrow \sin \theta)(\sin \varphi \hat{\mathbf{x}} + \cos \varphi \hat{\mathbf{y}}), \quad (12)$$

and

$$\Theta = \frac{|\bar{\sigma}_{xy}^\uparrow| \sin \theta}{\bar{\sigma}_{xx} \sin^2 \theta \cos^2 \varphi + \bar{\sigma}_{yy} \sin^2 \theta \sin^2 \varphi + \bar{\sigma}_{zz} \cos^2 \theta}. \quad (13)$$

From Eq. (12), we see that $\hat{\mathbf{J}}_s$ is always in the $x-y$ plane and $\hat{\mathbf{J}}_s$ is perpendicular to $\hat{\mathbf{n}}$ for $\hat{\mathbf{n}}||\hat{\mathbf{x}}$ and $\hat{\mathbf{n}}||\hat{\mathbf{y}}$. From Eq. (13), the extrema of Θ can be examined analytically from $\partial\Theta/\partial\theta = 0$

and $\partial\Theta/\partial\varphi = 0$, which yields the following stationary points

$$\begin{aligned} &(\frac{\pi}{2}, 0), (\frac{\pi}{2}, \pi), (\frac{\pi}{2}, \frac{\pi}{2}), (\frac{\pi}{2}, \frac{3\pi}{2}), \\ &(\theta_1, 0), (\pi - \theta_1, 0), (\theta_1, \pi), (\pi - \theta_1, \pi), \\ &(\theta_2, \frac{\pi}{2}), (\pi - \theta_2, \frac{\pi}{2}), (\theta_2, \frac{3\pi}{2}), (\pi - \theta_2, \frac{3\pi}{2}), \end{aligned} \quad (14)$$

where $\theta_{1,2}$ are defined as $\theta_1 \equiv \arcsin \sqrt{\bar{\sigma}_{zz}/(\bar{\sigma}_{xx} - \bar{\sigma}_{zz})}$, $\theta_2 \equiv \arcsin \sqrt{\bar{\sigma}_{zz}/(\bar{\sigma}_{yy} - \bar{\sigma}_{zz})}$. We substitute Eq. (14) into Eq. (13) and obtain the maximum value Θ_{max} by comparing Θ 's at different stationary points

$$\begin{aligned} \Theta_{max} &= \frac{|\bar{\sigma}_{xy}^\uparrow|}{\bar{\sigma}_{xx}}, \bar{\sigma}_{xx} \leq \bar{\sigma}_{yy} \leq 2\bar{\sigma}_{zz} \text{ or } \bar{\sigma}_{xx} \leq 2\bar{\sigma}_{zz} \leq \bar{\sigma}_{yy}, \\ \Theta_{max} &= \frac{|\bar{\sigma}_{xy}^\uparrow|}{\bar{\sigma}_{yy}}, \bar{\sigma}_{yy} \leq \bar{\sigma}_{xx} \leq 2\bar{\sigma}_{zz} \text{ or } \bar{\sigma}_{yy} \leq 2\bar{\sigma}_{zz} \leq \bar{\sigma}_{xx}, \\ \Theta_{max} &= \frac{|\bar{\sigma}_{xy}^\uparrow|}{2\bar{\sigma}_{zz}} \sqrt{\frac{\bar{\sigma}_{zz}}{\bar{\sigma}_{xx} - \bar{\sigma}_{zz}}}, \bar{\sigma}_{yy} > \bar{\sigma}_{xx} > 2\bar{\sigma}_{zz}, \\ \Theta_{max} &= \frac{|\bar{\sigma}_{xy}^\uparrow|}{2\bar{\sigma}_{zz}} \sqrt{\frac{\bar{\sigma}_{zz}}{\bar{\sigma}_{yy} - \bar{\sigma}_{zz}}}, \bar{\sigma}_{xx} > \bar{\sigma}_{yy} > 2\bar{\sigma}_{zz}. \end{aligned} \quad (15)$$

For the SPG $2^4/1m$, the conductivity components $\bar{\sigma}_{xx}$, $\bar{\sigma}_{yy}$ and $\bar{\sigma}_{xy}$ are spin polarized[41]. A similar argument gives rise to

$$\hat{\mathbf{J}}_s = -\text{sgn}(\sin \theta) \frac{[(\bar{\sigma}_{xx}^\uparrow - \bar{\sigma}_{xx}^\downarrow) \cos \varphi + 2\bar{\sigma}_{xy}^\uparrow \sin \varphi] \hat{\mathbf{x}} + [2\bar{\sigma}_{xy}^\uparrow \cos \varphi - (\bar{\sigma}_{xx}^\uparrow - \bar{\sigma}_{xx}^\downarrow) \sin \varphi] \hat{\mathbf{y}}}{\sqrt{(\bar{\sigma}_{xx}^\uparrow - \bar{\sigma}_{xx}^\downarrow)^2 + 4(\bar{\sigma}_{xy}^\uparrow)^2}}, \quad (16)$$

and

$$\Theta = \frac{\sqrt{(\bar{\sigma}_{xx}^\uparrow - \bar{\sigma}_{xx}^\downarrow)^2 + 4(\bar{\sigma}_{xy}^\uparrow)^2} \sin \theta}{2(\bar{\sigma}_{xx} \sin^2 \theta + \bar{\sigma}_{zz} \cos^2 \theta)}. \quad (17)$$

Equation (16) suggests that the spin current is always in the $x-y$ plane. As distinct from the SPGs $2^2/2m$ and $2^2m^2m^1m$,

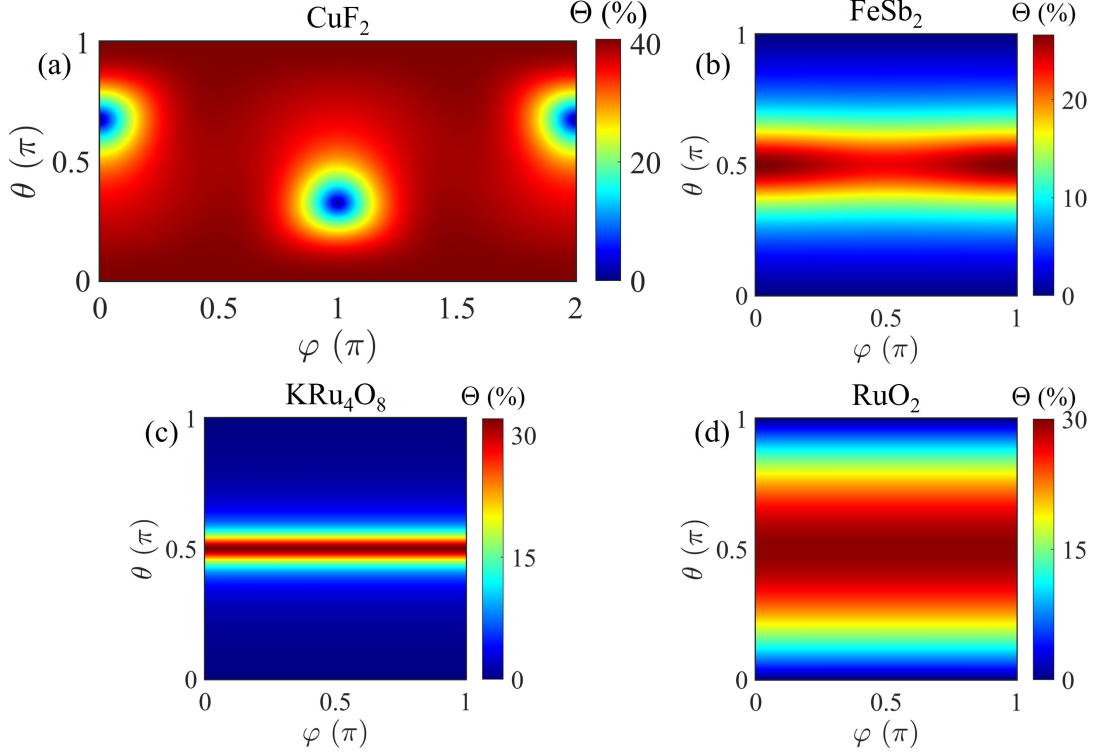


FIG. 1. Anisotropic charge-to-spin conversion ratio Θ at the Fermi energy as a function of (θ, φ) for the CuF_2 (a), FeSb_2 (b), $\text{K}_2\text{Ru}_8\text{O}_{16}$ (c), and RuO_2 (d). Note that, the Fermi energy for the semiconductor CuF_2 is at the 0.1 eV below the valence band maximum.

Θ is only dependent on θ , as seen from Eq. (17). We then find the following stationary points from $\partial\Theta/\partial\theta = 0$

$$\theta = \frac{\pi}{2}, \arcsin \sqrt{\frac{\bar{\sigma}_{zz}}{\bar{\sigma}_{xx} - \bar{\sigma}_{zz}}}, \pi - \arcsin \sqrt{\frac{\bar{\sigma}_{zz}}{\bar{\sigma}_{xx} - \bar{\sigma}_{zz}}}. \quad (18)$$

We use Eqs. (17) and (18) and find, with the same substitutions,

$$\begin{aligned} \Theta_{max} &= \frac{\sqrt{(\bar{\sigma}_{xx}^\uparrow - \bar{\sigma}_{xx}^\downarrow)^2 + 4(\bar{\sigma}_{xy}^\uparrow)^2}}{2\bar{\sigma}_{xx}}, \bar{\sigma}_{xx} \leq 2\bar{\sigma}_{zz}, \\ \Theta_{max} &= \sqrt{\frac{(\bar{\sigma}_{xx}^\uparrow - \bar{\sigma}_{xx}^\downarrow)^2 + 4(\bar{\sigma}_{xy}^\uparrow)^2}{16\bar{\sigma}_{zz}(\bar{\sigma}_{xx} - \bar{\sigma}_{zz})}}, \bar{\sigma}_{xx} > 2\bar{\sigma}_{zz}. \end{aligned} \quad (19)$$

For the SPG $^{24/1}m^2m^1m$, only $\bar{\sigma}_{xy}$ is spin polarized[41]. We substitute in Eqs. (7) and (8) and find

$$\hat{\mathbf{J}}_s = -\text{sgn}(\bar{\sigma}_{xy}^\uparrow \sin \theta)(\sin \varphi \hat{\mathbf{x}} + \cos \varphi \hat{\mathbf{y}}), \quad (20)$$

and

$$\Theta = \frac{|\bar{\sigma}_{xy}^\uparrow| \sin \theta}{\bar{\sigma}_{xx} \sin^2 \theta + \bar{\sigma}_{zz} \cos^2 \theta}, \quad (21)$$

which is φ independent. We see that Eq. (20) is the same with Eq. (12) due to the same nonzero spin conductivity component σ_{xy}^i between the SPGs $^{2m^2m^1m}$ and $^{24/1}m^2m^1m$.

Imposing the condition $\partial\Theta/\partial\theta = 0$ yields the following stationary points

$$\theta = \frac{\pi}{2}, \arcsin \sqrt{\frac{\bar{\sigma}_{zz}}{\bar{\sigma}_{xx} - \bar{\sigma}_{zz}}}, \pi - \arcsin \sqrt{\frac{\bar{\sigma}_{zz}}{\bar{\sigma}_{xx} - \bar{\sigma}_{zz}}}. \quad (22)$$

In this case, Θ_{max} can be obtained as

$$\begin{aligned} \Theta_{max} &= \frac{|\bar{\sigma}_{xy}^\uparrow|}{\bar{\sigma}_{xx}}, \bar{\sigma}_{xx} \leq 2\bar{\sigma}_{zz}, \\ \Theta_{max} &= \frac{|\bar{\sigma}_{xy}^\uparrow|}{2\bar{\sigma}_{zz}} \sqrt{\frac{\bar{\sigma}_{zz}}{\bar{\sigma}_{xx} - \bar{\sigma}_{zz}}}, \bar{\sigma}_{xx} > 2\bar{\sigma}_{zz}. \end{aligned} \quad (23)$$

IV. DFT RESULTS

Having demonstrated the anisotropic charge-to-spin conversion in d -wave altermagnets based on the general group-theoretical analysis, we now exemplify those phenomena in representative altermagnets based on the DFT calculations[42–46]. It should be noted that the computational details for the spin-resolved conductivity calculations including the lattice parameters, energy cutoff, k -point mesh and Hubbard- U values etc. are exactly the same as the previous work[41]. The more information concerning the magnetic structure, band structure, spin splitting, etc. should consult Ref. [41]. Similarly, we consider one candidate material for each d -wave SPG, as listed in the last column of Table I. To be specific, we consider the monoclinic CuF_2 (SPG

$2^2/2m$), the orthorhombic FeSb_2 (SPG $2^2m^2m^1m$), the tetragonal $\text{K}_2\text{Ru}_8\text{O}_{16}$ (SPG $2^4/1m$) and the tetragonal RuO_2 (SPG $2^4/1m^2m^1m$). Given the fact the CuF_2 is a wide-gap semiconductor while the other three candidates are metallic, we assume that the Fermi energy is at the 0.1 eV below the valence band maximum for CuF_2 . It is also worth noting here that although the presence of magnetic order in the RuO_2 is highly controversial[47, 48], we will, however, consider here the RuO_2 as an illustration of group-theoretical results.

Figure 1 shows the anisotropic charge-to-spin conversion ratio Θ at the Fermi energy as a function of (θ, φ) . It has to be stressed that Fig. 1 was produced by using $\Theta(\theta, \varphi)$ formulas given by Eqs. (11), (13), (17) and (21), where the spin-polarized conductivity $\bar{\sigma}_{ij}^\uparrow$ was calculated under the relaxation time approximation. For the monoclinic CuF_2 shown in Fig. 1(a), it is indicated that Θ reveals large values of more than 40% in a large area of the $\theta - \varphi$ plane except for three small regions with rather small values. This is to be expected since both the in-plane component $\bar{\sigma}_{xy}^\uparrow$ and the out-of-plane one $\bar{\sigma}_{yz}^\uparrow$ contribute to Θ , as seen from Eq. (11). For the orthorhombic FeSb_2 shown in Fig. 1(b), Θ is significant around $\theta = \pi/2$, i.e. electric field along the in-plane direction. This is legitimate since only the in-plane spin conductivity component σ_{xy}^i is symmetry allowed. In addition, Θ reaches the maximum value at $(\pi/2, 0)$ and $(\pi/2, \pi)$. This is due to the fact that $\bar{\sigma}_{xx} < \bar{\sigma}_{yy} < 2\bar{\sigma}_{zz}$ at the Fermi energy. As a result, we have $\Theta_{max} = |\bar{\sigma}_{xy}^\uparrow|/\bar{\sigma}_{xx} \sim 26.6\%$ at $(\pi/2, 0)$ and $(\pi/2, \pi)$, as seen from Eq. (15). Figure 1(c) shows $\Theta(\theta, \varphi)$ for the tetragonal $\text{K}_2\text{Ru}_8\text{O}_{16}$. As distinct from CuF_2 and FeSb_2 , Θ is φ independent as seen from Eq. (17). Since we have $\bar{\sigma}_{xx} < 2\bar{\sigma}_{zz}$ at the Fermi energy, Θ reaches its maximum of more than 30% at $\theta = \pi/2$ according to Eq. (19). A particularly noteworthy conversion ratio is centered on $\theta = \pi/2$ and Θ decays rapidly as θ is away from $\pi/2$. This is so because all the symmetry allowed spin conductivity components σ_{xx}^i , σ_{yy}^i and σ_{xy}^i are in-plane, which would expect to suppress the out-of-plane spin current. Figure 1(d) shows $\Theta(\theta, \varphi)$ for the tetragonal RuO_2 . It is seen that Θ is φ independent similar to that for the $\text{K}_2\text{Ru}_8\text{O}_{16}$. According to Eq. (23), since $\bar{\sigma}_{xx} < 2\bar{\sigma}_{zz}$ at the Fermi energy, we have $\Theta_{max} = |\bar{\sigma}_{xy}^\uparrow|/\bar{\sigma}_{xx} \sim 29.5\%$ at $\theta = \pi/2$. This value is quite

similar to previous work[21, 49]. Another feature is that $\Theta(\theta)$ is rather broadening around $\theta = \pi/2$, contrary to that for the $\text{K}_2\text{Ru}_8\text{O}_{16}$ (Fig. 1(c)). This illustrates the point that a large charge-to-spin conversion ratio can be achieved even if the charge current deviates greatly from the in-plane direction.

V. DISCUSSION AND SUMMARY

Note that the SOC is ignored since we focus on the nonrelativistic charge-to-spin conversion in this work. However, the effect of SOC on the conversion ratio would be negligible[21]. For example, the maximum conversion ratio at the Fermi energy for the FeSb_2 with SOC is $\sim 27.4\%$ quite similar to that of $\sim 26.6\%$ without SOC. By considering the SOC, there are additional nonzero spin conductivity components in addition to those listed in Table I. In such cases, it will usually be convenient to dictate the spin conductivity by use of the magnetic point group[21, 37]. Second, our derived anisotropic charge-to-spin conversion formulas for bulk altermagnets can be extended to be applicable to two-dimensional altermagnets[50–52], for which we have $\theta = \pi/2$ and the conversion anisotropy is described by φ .

In summary, we have investigated the anisotropic nonrelativistic charge-to-spin conversion in altermagnets based on the group-theoretical analysis and DFT calculations. We show that the charge-to-spin conversion efficiency is highly anisotropic for current along different crystal orientations. In particular, we derive the analytical expression of the anisotropic charge-to-spin conversion ratio and identify the maximum conversion efficiency. Our results are expected to pave the practical way to produce the high charge-to-spin conversion efficiency in altermagnets.

ACKNOWLEDGMENTS

This research was supported by the National Natural Science Foundation of China (Grant No. 12274102).

DATA AVAILABILITY

The data that support the findings of this article are available from the authors upon reasonable request.

-
- [1] J. Sinova, S. O. Valenzuela, J. Wunderlich, C. H. Back, and T. Jungwirth, Spin Hall effects, *Rev. Mod. Phys.* **87**, 1213 (2015).
 - [2] A. Soumyanarayanan, N. Reyren, A. Fert, and C. Panagopoulos, Emergent phenomena induced by spin-orbit coupling at surfaces and interfaces, *Nature* **539**, 509 (2016).
 - [3] W. Han, Y. Otani, and S. Maekawa, Quantum materials for spin and charge conversion, *npj Quant. Mater.* **3**, 27 (2018).
 - [4] F. Trier, P. Noël, J. Kim, J. Attané, L. Vila, and M. Bibes, Oxide spin-orbitronics: spin–charge interconversion and topological spin textures, *Nat. Rev. Mater.* **7**, 258 (2022).
 - [5] J. C. Slonczewski, Current-driven excitation of magnetic multilayers, *J. Magn. Magn. Mater.* **159**, L1 (1996).
 - [6] L. Berger, Emission of spin waves by a magnetic multilayer

- traversed by a current, *Phys. Rev. B* **54**, 9353 (1996).
- [7] J. A. Katine, F. J. Albert, R. A. Buhrman, E. B. Myers, and D. C. Ralph, Current-Driven Magnetization Reversal and Spin-Wave Excitations in Co/Cu/Co Pillars, *Phys. Rev. Lett.* **84**, 3149 (2000).
- [8] A. Brataas, A. D. Kent, and H. Ohno, Current-induced torques in magnetic materials, *Nat. Mater.* **11**, 372 (2012).
- [9] A. Manchon and S. Zhang, Theory of nonequilibrium intrinsic spin torque in a single nanomagnet, *Phys. Rev. B* **78**, 212405 (2008).
- [10] A. Manchon and S. Zhang, Theory of spin torque due to spin-orbit coupling, *Phys. Rev. B* **79**, 094422 (2009).
- [11] A. Matos-Abiad and R. L. Rodríguez-Suárez, Spin-orbit cou-

- pling mediated spin torque in a single ferromagnetic layer, *Phys. Rev. B* **80**, 094424 (2009).
- [12] I. M. Miron, K. Garello, G. Gaudin, P. J. Zermatten, M. V. Costache, S. Auffret, S. Bandiera, B. Rodmacq, A. Schuhl, and P. Gambardella, Perpendicular switching of a single ferromagnetic layer induced by in-plane current injection, *Nature (London)* **476**, 189 (2011).
- [13] L. Liu, C. F. Pai, Y. Li, H. W. Tseng, D. C. Ralph, and R. A. Buhrman, Spin-torque switching with the giant spin Hall effect of tantalum, *Science* **336**, 555 (2012).
- [14] L. Liu, O. J. Lee, T. J. Gudmundsen, D. C. Ralph, and R. A. Buhrman, Current-Induced Switching of Perpendicularly Magnetized Magnetic Layers Using Spin Torque from the Spin Hall Effect, *Phys. Rev. Lett.* **109**, 096602 (2012).
- [15] A. Manchon, J. Železný, I. M. Miron, T. Jungwirth, J. Sinova, A. Thiaville, K. Garello, and P. Gambardella, Current-induced spin-orbit torques in ferromagnetic and antiferromagnetic systems, *Rev. Mod. Phys.* **91**, 035004 (2019).
- [16] X. Han, X. Wang, C. Wang, G. Yu, X. Lv, Spin-orbit torques: Materials, physics, and devices, *Appl. Phys. Lett.* **118**, 120502 (2021).
- [17] C. Song, R. Zhang, L. Liao, Y. Zhou, X. Zhou, R. Chen, Y. You, X. Chen, and F. Pan, Spin-orbit torques: Materials, mechanisms, performances, and potential applications, *Prog. Mater. Sci.* **118**, 100761 (2021).
- [18] R. H. Silsbee, Spin-orbit induced coupling of charge current and spin polarization, *J. Phys.: Condens. Matter* **16**, R179 (2004).
- [19] L. L. Tao and E. Y. Tsymlar, Spin-orbit dependence of anisotropic current-induced spin polarization, *Phys. Rev. B* **104**, 085438 (2021).
- [20] M.-G. Kang, S. Lee, and B.-G. Park, Field-free spin-orbit torques switching and its applications, *npj Spintronics* **3**, 8 (2025).
- [21] R. González-Hernández, L. Šmejkal, K. Výborný, Y. Yahagi, J. Sinova, T. Jungwirth, and J. Železný, Efficient Electrical Spin Splitter Based on Nonrelativistic Collinear Antiferromagnetism, *Phys. Rev. Lett.* **126**, 127701 (2021).
- [22] L. Šmejkal, J. Sinova, and T. Jungwirth, Beyond Conventional Ferromagnetism and Antiferromagnetism: A Phase with Non-relativistic Spin and Crystal Rotation Symmetry, *Phys. Rev. X* **12**, 031042 (2022).
- [23] L. Šmejkal, J. Sinova, and T. Jungwirth, Emerging Research Landscape of Altermagnetism, *Phys. Rev. X* **12**, 040501 (2022).
- [24] L. Bai, W. Feng, S. Liu, L. Šmejkal, Y. Mokrousov, Y. Yao, Altermagnetism: Exploring New Frontiers in Magnetism and Spintronics, *Adv. Funct. Mater.* **34**, 2409327 (2024).
- [25] S. S. Fender, O. Gonzalez, and D. K. Bediako, Altermagnetism: A Chemical Perspective, *J. Am. Chem. Soc.* **147**, 2257 (2025).
- [26] C. Song, H. Bai, Z. Zhou, L. Han, H. Reichlova, J. Hugo Dil, J. Liu, X. Chen, and F. Pan, Altermagnets as a new class of functional materials, *Nat. Rev. Mater.* **10**, 473 (2025).
- [27] S. Hayami, Y. Yanagi, and H. Kusunose, Momentum-Dependent Spin Splitting by Collinear Antiferromagnetic Ordering, *J. Phys. Soc. Jpn.* **88**, 123702 (2019).
- [28] L.-D. Yuan, Z. Wang, J.-W. Luo, E. I. Rashba, and A. Zunger, Giant momentum-dependent spin splitting in centrosymmetric low-Z antiferromagnets, *Phys. Rev. B* **102**, 014422 (2020).
- [29] H. Bai, L. Han, X. Y. Feng, Y. J. Zhou, R. X. Su, Q. Wang, L. Y. Liao, W. X. Zhu, X. Z. Chen, F. Pan, X. L. Fan, and C. Song, Observation of Spin Splitting Torque in a Collinear Antiferromagnet RuO_2 , *Phys. Rev. Lett.* **128**, 197202 (2022).
- [30] S. Karube, T. Tanaka, D. Sugawara, N. Kadoguchi, M. Kohda, and J. Nitta, Observation of Spin-Splitter Torque in Collinear Antiferromagnetic RuO_2 , *Phys. Rev. Lett.* **129**, 137201 (2022).
- [31] Y. Zhang, H. Bai, J. Dai, L. Han, C. Chen, S. Liang, Y. Cao, Y. Zhang, Q. Wang, W. Zhu, F. Pan, and C. Song, Electrical manipulation of spin splitting torque in altermagnetic RuO_2 , *Nat. Commun.* **16**, 5646 (2025).
- [32] F. Freimuth, S. Blügel, and Y. Mokrousov, Anisotropic Spin Hall Effect from First Principles, *Phys. Rev. Lett.* **105**, 246602 (2010).
- [33] B. Lao, P. Liu, X. Zheng, Z. Lu, S. Li, K. Zhao, L. Gong, T. Tang, K. Wu, Y.-g. Shi, Y. Sun, X.-Q. Chen, R.-W. Li, and Z. Wang, *Phys. Rev. B* **106**, L220409 (2022).
- [34] L. Salemi and P. M. Oppeneer, Theory of magnetic spin and orbital Hall and Nernst effects in bulk ferromagnets, *Phys. Rev. B* **106**, 024410 (2022).
- [35] F. Freimuth, S. Blügel, and Y. Mokrousov, Spin-orbit torques in Co/Pt(111) and Mn/W(001) magnetic bilayers from first principles, *Phys. Rev. B* **90**, 174423 (2014).
- [36] M. Kimata, H. Chen, K. Kondou, S. Sugimoto, P. K. Muduli, M. Ikhlas, Y. Omori, T. Tomita, Allan. H. MacDonald, S. Nakatsuji, and Y. Otani, Magnetic and magnetic inverse spin Hall effects in a non-collinear antiferromagnet, *Nature* **565**, 627 (2019).
- [37] K. Tenzin, B. Kilic, R. M. Sattigeri, Z. He, C. C. Ye, M. Costa, M. B. Nardelli, C. Autieri, and J. Ślawińska, Persistent spin textures, altermagnetism and charge-to-spin conversion in metallic chiral crystals TM_3X_6 , *npj Spintronics* **3**, 46 (2025).
- [38] J. Callaway, *Quantum Theory of the Solid State*, (Academic Press, 1991).
- [39] X. Chen, Y. Fu, X. Wang, Yu Sui, H. J. Zhao, and L. L. Tao, Magnetic control of nonreciprocal charge transport, *Phys. Rev. B* **111**, 155411 (2025).
- [40] Q. Zhang, X. Chen, M. Dou, M. Ye. Zhuravlev, A. V. Nikolaev, X. Wang, and L. L. Tao, Anisotropic nonlinear transport in two-dimensional ferroelectrics, *Phys. Rev. B* **112**, 075422 (2025).
- [41] M. Dou, X. Wang, and L. L. Tao, Anisotropic spin-polarized conductivity in collinear altermagnets, *Phys. Rev. B* **111**, 224423 (2025).
- [42] D. Vanderbilt, Soft self-consistent pseudopotentials in a generalized eigenvalue formalism, *Phys. Rev. B* **41**, 7892(R) (1990).
- [43] P. Giannozzi, S. Baroni, N. Bonini, M. Calandra, R. Car, C. Cavazzoni, D. Ceresoli, G. L. Chiarotti, M. Cococcioni, I. Dabo *et al.*, QUANTUM ESPRESSO: a modular and open-source software project for quantum simulations of materials, *J. Phys.: Condens. Matter* **21**, 395502 (2009).
- [44] P. Giannozzi, O. Andreussi, T. Brumme, O. Bunau, M. B. Nardelli, M. Calandra, R. Car, C. Cavazzoni, D. Ceresoli, M. Cococcioni *et al.*, Advanced capabilities for materials modelling with Quantum ESPRESSO, *J. Phys.: Condens. Matter* **29**, 465901 (2017).
- [45] P. Giannozzi, O. Baseggio, P. Bonfà, D. Brunato, R. Car, I. Carnimeo, C. Cavazzoni, S. de Gironcoli, P. Delugas, F. F. Ruffino *et al.*, Quantum ESPRESSO toward the exascale, *J. Chem. Phys.* **152**, 154105 (2020).
- [46] J. P. Perdew, K. Burke, and M. Ernzerhof, Generalized Gradient Approximation Made Simple, *Phys. Rev. Lett.* **77**, 3865 (1996).
- [47] M. Hiraishi, H. Okabe, A. Koda, R. Kadono, T. Muroi, D. Hirai, and Z. Hiroi, Nonmagnetic Ground State in RuO_2 Revealed by Muon Spin Rotation, *Phys. Rev. Lett.* **132**, 166702 (2024).
- [48] J. Liu, J. Zhan, T. Li, J. Liu, S. Cheng, Y. Shi, L. Deng, M. Zhang, C. Li, J. Ding *et al.*, Absence of Altermagnetic Spin Splitting Character in Rutile Oxide RuO_2 , *Phys. Rev. Lett.* **133**, 176401 (2024).
- [49] W. Zhang, M. Zheng, Y. Liu, P. Zhang, Z. Zhang, R. Xiong, and Z. Lu, Unconventional spin Hall effect in rutile $\text{Cr}_{0.5}\text{X}_{0.5}\text{O}_2$

- ($X = \text{Ti, V, Os, Fe}$), Phys. Rev. B **110**, 214419 (2024).
- [50] J. Sødequist and T. Olsen, Two-dimensional altermagnets from high throughput computational screening: Symmetry requirements, chiral magnons, and spin-orbit effects, Appl. Phys. Lett. **124**, 182409 (2024).
- [51] Y. Che, H. Lv, X. Wu, and J. Yang, Realizing altermagnetism in two-dimensional metal-organic framework semiconductors with electric-field-controlled anisotropic spin current, Chem. Sci. **15**, 13853 (2024).
- [52] Y. Che, Y. Chen, X. Liu, H. Lv, X. Wu, and J. Yang, Inverse Design of 2D Altermagnetic Metal-Organic Framework Monolayers from Hückel Theory of Nonbonding Molecular Orbitals, JACS Au **5**, 381 (2025).